Determining the Origin of the Stabilization of DNA by 5-Aminopropynylation of Pyrimidines†

James Booth,‡,§ Tom Brown,‡ Sunil J. Vadhia,‡ Oliver Lack,‡ W. Jon Cummins,|| John O. Trent,⊥ and Andrew N. Lane*,⊥

School of Chemistry, University of Southampton, Highfield, Southampton SO17 1BJ, U.K., GE Healthcare, Grove Center, White Lion Road, Amersham, Bucks HP7 9LL, U.K., and J. G. Brown Cancer Center, University of Louisville, Louisville, Kentucky 40202

Received November 19, 2004; Revised Manuscript Received January 22, 2005

ABSTRACT: DNA duplexes are stabilized by aminopropynyl modification of pyrimidines at the 5 position. A combination of thermodynamic analyses as a function of ionic strength, NMR, and molecular modeling has been applied to determine the origin of the stabilization. UV melting studies of a dodecamer bearing one, two, or three nonadjacent modified dU and dC and of a single dU(8) in the Dickerson−Drew dodecamer revealed that the modifications are essentially additive in terms of T_m, ΔG, and ΔH, and there is little difference between dU and dC. The free energy change was parsed into electrostatic and nonelectrostatic components, which showed a significant contribution from charge interactions at physiological ionic strength but also a nonelectrostatic contribution that arises in part from hydration. NMR spectroscopy of the modified Dickerson−Drew dodecamer revealed that the conformation of the duplexes is not significantly altered by the modifications, though ^{31}P NMR shows that the positive charge may affect ionic interactions with the oxygen atoms of the neighboring phosphates. The modified duplex showed significant hydration in both major and minor grooves. The single strands were also analyzed by NMR, which showed evidence of significant stacking interactions in the modified oligonucleotide. Parsing the energy contribution has shown that electrostatics and hydration can produce substantial increases in thermodynamic stability without significant changes in the conformation of the duplex state. These considerations have significance for the design of oligonucleotides used for hybridization.

Chemical modification of nucleic acids is an area of intense interest both as a means to understanding the origins of stability of nucleic acids and for biotechnological purposes in improving the thermodynamic and biochemical properties of oligonucleotides that may be used therapeutically (*1*, *2*).

There are many possibilities for chemically modifying nucleic acids without disrupting the specific base pairing, including sites on the bases, on the sugars, or on the phosphates. Ideally, it is desirable to change physical properties such as enhanced thermodynamic stability, maintain good solubility in different solvents, and decrease susceptibility to nucleases. We have been developing modifications of the bases, particularly at the 5 position of pyrimidines, with a view to stabilizing duplexes and triple helices (*3*−*7*).

One particularly promising base modification is the propyne group at the C5 of pyrimidines. This has been shown to have a strong stabilizing effect on DNA·RNA hybrids (*3*−*7*) and on DNA triple helices (*8*−*12*). Additional functionalization of the propyne group leads to further stabilization. For example, the aminopropynyl group clearly increases the stability of duplexes and triplexes significantly, presumably by additional electrostatic interactions (*8*, *12*). However, a detailed parsing of the free energy of stabilization of nucleic acids bearing such modifications has not been reported, so the true origins of the effect remain speculative. To optimize future synthetic efforts, we have undertaken an extensive thermodynamic and conformational analysis of the stabilization of DNA duplexes by aminopropynyl modifications.

There are numerous possibilities to account for the observed stabilization, including effects of the modification on major groove hydration, changes in stacking energies due to alteration of the electronic structures of the modified bases, electrostatic interactions between the charged modifications and the phosphodiester backbone, and differences in structure of the component strands (e.g., preorganization). We have designed experiments and computational strategies to test these possibilities. We are able to show the amino group does indeed impart a favorable electrostatic interaction, and we are able to quantify this contribution as a function of ionic strength. We have also determined the conformational and hydration properties of duplexes bearing different modifications using high-resolution NMR spectroscopy and molecular modeling techniques. As we are interested in

† This work was supported by NSF-EPSCoR for the purchase of the 18.8 T NMR spectrometer (to R. J. Wittebort), the J. G. Brown Cancer Center, and the Kentucky Challenge for Excellence (ANL). J.B. gratefully acknowledges a BBSRC CASE studentship−Amersham.

* Corresponding author. Tel: 502 8523067. E-mail: anlane01@louisville.edu. Fax: 502 8524311.

‡ University of Southampton.

§ Present address: Section for Cellular and Genetic Therapy, Institute of Microbiology, Rikshospitalet, Forskningsparken, Gaustadalleen 21, 0349 Oslo, Norway.

|| GE Healthcare.

⊥ University of Louisville.

10.1021/bi047561d CCC: $30.25
Published on Web 02/25/2005

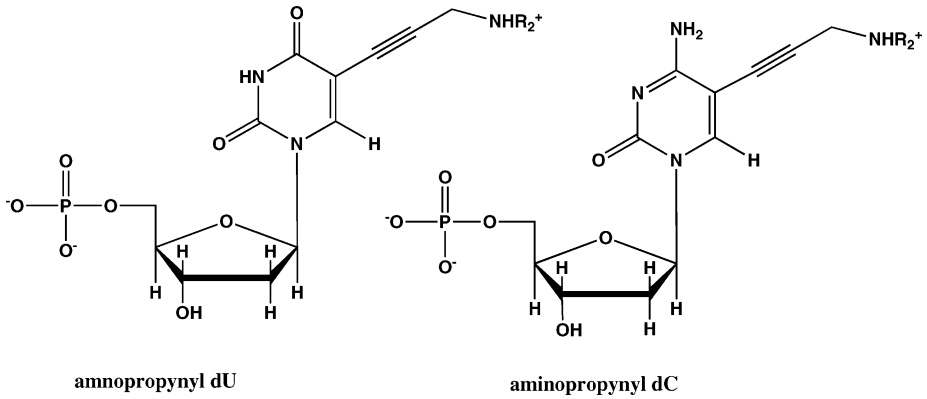

FIGURE 1: Chemical structures of the modified nucleotides: R = H, aminopropynyl; R = CH_3, dimethylaminopropynyl.

thermodynamic stability, we have also examined the influence of the modifications on the single strands.

MATERIALS AND METHODS

Materials

DNA Synthesis and Purification. The modified nucleotides (Figure 1) were prepared as follows: 5-aminopropynyl-dU was synthesized using either 2,2,2-trifluoro-*N*-(prop-2-ynyl)-acetamide (*13*) or 3-phthalimido-1-propyne (*14*, *15*). Dimethylaminopropynyl-dU was synthesized according to ref *16* using 3-(*N*-dimethylamino)-1-propyne. Aminopropynyl-dC was synthesized as described (*15*). The dimethylaminopropynyl-dC nucleoside is novel and was synthesized as described in the Supporting Information.

All oligonucleotides were synthesized on an ABI 394 DNA synthesizer using a standard 1.0 mmol phosphoramidite cycle (four syntheses per oligonucleotide). Cleavage from the solid support and deprotection were carried out using 10% methylamine in water (2 mL) containing phenol (5 mg) for 36 h at room temperature. Products were purified by reversed-phase HPLC [column: ABI C8 (octyl), 8 mm × 250 mm, pore size = 300 Å] (buffer A, 0.1 M ammonium acetate, pH 7.0; buffer B, 0.1 M ammonium acetate with 20% acetonitrile, pH 7.0). Gradient time in minutes (% buffer B): 0 (0); 3 (0); 5 (20); 21 (100); 25 (100); 27 (0); 30 (0). UV detection was at 290 nm. Mass data were obtained for all oligonucleotides using a MALDI-TOF ThermoBioAnalysis Dynamo mass spectrometer in positive ion mode using a 3-hydroxypicolinic acid/picolinic acid (4:1) matrix with 50% aqueous acetonitrile solvent.

The following strands were prepared for thermodynamic and NMR analyses: (1) d(G1C2T3A4T5C6T7A8T9C10T11G12) (positions were modified at T7, T7 + T9, and T7 + T9 + T5 with either aminopropynyl- or dimethylaminopropynyl-dU and separately at C6, C6 + C2, and C6 + C2 + C10 with either aminopropynyl- or dimethylaminopropynyl-dC); (2) d(C1A2G3A4T5A6G7A8T9A10G11C12); (3) d(CGCGAATT*CGCG)$_2$ (where T* is either aminopropynyl- or dimethylaminopropynyl-dU).

Methods

Thermodynamics. All UV melting experiments were carried out in a Cary 400 UV/visible spectrometer with a Cary Peltier temperature controller. The standard buffer was 0.1 M NaCl, 0.001 M EDTA, and 0.01 M sodium phosphate, pH 7.0. The influence of ionic strength was determined by systematically changing the concentration of NaCl in the solution, under otherwise constant buffer conditions.

The thermodynamic parameters were determined in two ways. First, at constant ionic strength, in the standard buffer conditions, the T_m was estimated from the maximum in the first derivative curve, d*A*/d*T*, as a function of strand concentration. For dodecamers, the error involved in measuring T_m by this method is small, as verified by independent curve-fitting methods (see below). The ΔH and ΔS values were then obtained by van't Hoff analysis according to

$$1/T_m = \Delta S/\Delta H - (R/\Delta H)\ln[rs_t] \quad (1)$$

where s_t is the strand concentration and r is unity for self-complementary duplexes and 0.25 for noncomplementary duplexes. ΔH and ΔS determined by this method were in good agreement with the values obtained by curve fitting.

ΔC_p is implicitly assumed to be zero in eq 1. The value of ΔC_p per base pair has been variously estimated to be in the range 40−80 cal/(mol·K) (*17*−*22*). Over a moderate range of temperatures, the enthalpy determined from the van't Hoff plot (eq 1) is equivalent to the enthalpy at the middle of the range. However, for the extended temperature range encountered over a wide range of salt concentration, the nonzero value of ΔC_p may need to be considered (*4*).

In addition, complete melting curves were analyzed using Meltwin (*23*) and software written in-house, using sloping baselines to obtain optimal agreement with the data.

$$A(260) = 0.5\epsilon_D s_t + \Delta\epsilon s \quad (2)$$

where ϵ_D is the absorption coefficient of the duplex, ϵ_S is the absorption coefficient of the strands, s_t is the total strand concentration, s is the strand concentration, and $\Delta\epsilon$ is the difference absorption coefficient. At high salt concentration (e.g., 1 M), the pre- and posttransition baselines are essentially flat. However, at lower concentrations of salt, the baselines have a significant slope, and therefore additional terms are required to fit the optical data reliably.

The dissociation constant

$$K = s_A s_B/d \quad (3)$$

For $s_A = s_B$, the strand concentration, s, is

$$s = 0.25(-K + [K^2 + 8Kst]^{0.5}) \quad (4)$$

and

$$K(T) = K^0 \exp(\Delta H/R(1/T - 1/T^0)) \quad (5)$$

where T is a reference temperature, e.g., the T_m.

All model fitting implicitly assumes a two-state melting process. Good agreement was obtained for the two methods of data analysis. The curve-fitting method was then used to determine the influence of salt concentration on stability at a fixed concentration of DNA duplex. Errors were estimated from the nonlinear regression analysis.

We aim to parse the free energy and its components into the polyelectrolyte and nonpolyelectrolyte effects by varying the ionic strength. The modified bases are expected to bear a net positive charge at pH 7, as the pK of the aminopropynyl group should be >8, and this will be raised by interaction with the negative charge of the phosphates (see below).

The influence of ionic strength was assessed using the Record formalism (*24*−*26*). Briefly, the melting temperature is expected to increase with increasing ionic strength because of a combination of ion condensation and ionic strength effects, which is purely entropic in origin. Thus

$$\partial(1/T_m)/\partial \ln(I) = (R/\Delta H^\circ)(N/2)[(1/\zeta s - 1)/\zeta d] \quad (6)$$

where $\zeta s,d = e^2/\epsilon kTr_{s,d}$ are the condensation parameters for single strands and duplex, respectively, and N is the number of phosphates (22 for a dodecamer duplex). e is the electronic charge, ϵ is the dielectric permittivity, k is Boltzmann's constant, and r is the axial rise. For a B-DNA-coil transition, $[(1/\zeta s - 1)/\zeta d] \approx 0.27$ at 310 K.

This provides estimates of the number of charges involved in the transition, which should differ for the aminopropynyl-modified duplexes as these groups bear a positive charge. This formalism was developed for long uniform polymers, which clearly does not apply exactly to a short DNA sequence. Recently, the end effects for oligonucleotides have been analyzed (*27*); for DNA duplexes of >10 bp, the apparent number of charges is around 10% lower than for an infinite polyelectrolyte. Hence, for estimating the inclusion of positive charges into the same duplex, i.e., changes in electrostatics, this formalism is adequate. It also indicates that the derived electrostatic contribution should be entirely entropic. To the extent that the two-state transition is not obeyed at low ionic strength, there may also be ionic strength effects on enthalpy changes as well as on entropy changes.

The distinction between nonelectrostatic and polyelectrolyte effects is easiest to make at 1 M salt, where all of the electrostatics effects are shielded. The value of ΔG at 1 M salt is the nonpolyelectrolyte contribution, and the difference between this value and that at any other ionic strength (but the same temperature) is the polyelectrolyte contribution at that ionic strength. Hence one might expect smaller differences in ΔG at 1 M salt for the unmodified and modified duplexes than at lower ionic strength where the electrostatic contributions are relatively more important. However, it should be noted that at high salt concentrations, e.g., 1 M, the water activity is less than 55.5 M because the ions are solvated. Because the duplex/strand transition is associated with a change in hydration, the high salt concentration may also affect the equilibrium through changes in water activity (*24*, *28*). In this instance, extrapolation from lower salt concentration to 1 M may give a less biased estimate of the polyelectrolyte effects, and the deviation between the extrapolated value and the observed value at 1 M salt may give an indication of the importance of hydration differences between the duplex and strand states.

The dissociation constant for a duplex can be written as

$$K = (a_{s1}a_{s2}/a_D)a_w{}^n a_M{}^k \quad (7)$$

n is the number of water molecules released, k is the number of counterions released on dissociation, a_{s1}, a_{s2}, a_D, a_w, and a_M are the activities of strands 1 and 2, the DNA duplex, water, and cation, respectively. If the dissociation constant is measured in terms of concentrations, then the true dissociation constant

$$K = K_0 K_\gamma w^n m^k \gamma_w{}^n \gamma_M{}^k \quad (8)$$

where K_0 is the dissociation constant in terms of concentrations and K_γ is the ratio of the activity coefficients, γ, of the DNA duplex and strands.

As the concentration of sodium chloride is varied, the activity of the water and of the DNA is affected, and the dependence of the dissociation constant on the salt activity is

$$\partial \ln K/\partial \ln [Na^+] = \partial \ln K_\gamma/\partial \ln [Na^+] + n\,\partial \ln w/\partial \ln [Na^+] + n\,\partial \ln \gamma_w/\partial \ln [Na^+] + k\,\partial \ln \gamma_{Na}/\partial \ln [Na^+] \quad (9)$$

The first term on the right-hand side of eq 9 is the nonideality effect of salt on the DNA, the second term represents the decrease in water interaction due to replacement by salt, the third is the nonideality term from salt−water interactions, and the final term is the electrostatic salt−salt nonideality effect. The effect of salt on activities of solute and salt is accounted for by the Record−Manning condensation analysis (see above). The effect of salt on water activity can be accounted for if the water activity as a function of salt concentration is known. Fortunately, this has been tabulated, and the function is essentially linear up to >1 M sodium chloride with a slope $da_w/d[Na] = -0.049\ M^{-1}$. The remaining uncertainty then is the number of water molecules taken up on association. In polynucleotides, approximately 4 water molecules are released per base pair on unfolding (*28*). Thus about 48 waters should be taken up on forming the dodecamer duplex, indicating a rather strong dependence of the free energy on water activity. This effect counteracts the stabilization of the duplex by increasing salt concentration.

NMR Sample Preparation. HPLC-purified DNA was lyophilized for storage, then redissolved in phosphate buffer, pH 7, annealed from 90 °C, dialyzed against 0.1 M NaCl and 10 mM sodium phosphate, pH 7, lyophilized, and then brought to 10% D_2O + 0.05 mM DSS[1] (internal reference) for NMR analysis. NMR spectra were recorded at 14.1 or

[1] Abbreviations: DSS, 2,2′-dimethylsilapentanesulfonate; HSQC, heteronuclear single-quantum coherence; DQF-CSY, double-quantum-filtered correlation spectroscopy; NOE, nuclear Overhauser enhancement; TOCSY, total correlation spectroscopy; GB/SA, generalized Born/surface area; PRCG, Polak−Ribier conjugate gradient.

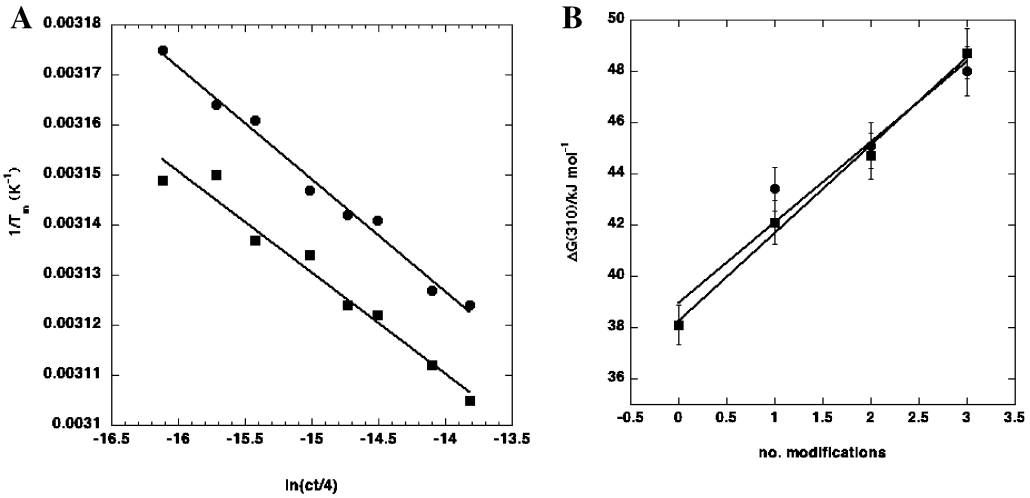

FIGURE 2: UV melting of modified duplexes. Oligonucleotide 1 duplex. (A) van't Hoff analysis of the aminopropynyl-modified duplex melting: (●) T5, T7, T9 modified; (■) C6 + C2 + C10 modified. (B) Dependence of $\Delta G(310)$ at 0.117 M Na^+ on the number of modifications: (●) T5, T7, T9 modified; (■) C6 + C2 + C10 modified.

18.8 T on four-channel Varian Inova spectrometers, using an inverse triple resonance probe (HCP at 14.1 T, triaxis pfg HCN at 18.8 T). NOESY and TOCSY spectra were recorded in H_2O (11 °C), after which the samples were lyophilized and redissolved in D_2O. NOESY spectra at two mixing times, DQF-COSY, and natural abundance C-13 HSQC + P-31 HSQC spectra were recorded on both samples (30 °C) using a 5 mm HCP probe. Similar experiments were carried out on the noncomplementary dodecamer strands with and without three dU modifications.

NMR spectra were assigned by standard approaches using TOCSY and NOESY experiments. Gradient $^{13}C-^{1}H$ HSQC and $^{31}P-^{1}H$ experiments were carried out at 14.1 T using a 5 mm HCP probe. Sugar conformations were determined using high-resolution DQF-COSY spectra and NOESY intensities for the H1′−H4′ NOE as previously described (*29*). Spectra of single- stranded dodecamers were acquired in a similar manner, but using longer mixing times in the NOESY experiments (500−800 ms). One-dimensional NMR spectra were recorded as a function of temperature to monitor changes in base stacking.

Hydration Experiments. Watergate NOESY and Watergate ROESY with mixing times of 50 ms/25 ms and 40 ms/20 ms at 5 °C, respectively, were recorded at both 14.1 and 18.8 T on the samples in 10% D_2O/90% H_2O, as previously described (*30*).

Molecular Modeling. The ecoR1 structure d(CGCGAATTCGCG)$_2$ was built using standard B-type DNA parameters within Macromodel 7.01 (*31*). The T8 bases were modified to include the protonated propargylamino or the dimethylpropargylamino group and minimized using the AMBER* force field (1000 steps steepest descents followed by 1000 steps PRCG conjugate gradient) with the GB/SA implicit water hydration approximation. The methyl−amine torsion bond was systematically driven 360 deg in 15 deg increments, with minimization as above at each position to find the low energy positions. The hydration model with a single water molecule bridging (i) or ($i - 1$) phosphate groups was manually added and minimized. Molecular dynamics simulations with an equilibration period of 50 ps (1.5 fs time step, 300 K) and a production period of 1 ns were performed for the (i) and ($i - 1$) propargylamino group and dimethylpropargylamino models unhydrated and with a single explicit water molecule using the above conditions.

Table 1: Thermodynamic Parameters for Noncomplementary Duplexes at 0.117 M Na^+ [a]

modification	no.	ΔH (kJ/mol)	ΔS [kJ/(mol·K)]	ΔG_{310} (kJ/mol)	T_m (2 μM) (K)
non	0	354 ± 7	1.02 ± 0.024	38.1 ± 0.3	310.7
U	1	390 ± 5	1.12 ± 0.014	43.4 ± 0.17	314.7
U	2	396 ± 5.9	1.13 ± 0.18	45.1 ± 0.33	315.6
U	3	403 ± 3	1.15 ± 0.009	48 ± 0.17	317.7
C	1	37 ± 2.7	1.07 ± 0.0086	42.1 ± 0.13	314
C	2	380 ± 2.9	1.083 ± 0.0089	44.7 ± 0.13	316.1
C	3	384 ± 3.9	1.08 ± 0.012	48.7 ± 0.17	319.8
dmU	1	381.0 ± 0.96	1.091 ± 0.003	42.7 ± 0.04	314.6
dmU	2	360 ± 1.3	1.02 ± 0.004	43.05 ± 0.04	315.0
dmU	3	355.4 ± 4.3	1.01 ± 0.013	43.5 ± 0.08	316.5
dmC	1	397 ± 4.6	1.02 ± 0.015	42.8 ± 0.13	316.5
dmC	2	382.6 ± 5.0	1.083 ± 0.015	46.6 ± 0.25	317.3
dmC	3	407.8 ± 5.3	1.16 ± 0.016	48.9 ± 0.21	319.8

[a] Parameters were determined as described in the text. dmU and dmC are dimethylaminopropynyl derivatives of U and C, respectively. Errors were estimated from replicate experiments (four replicates).

RESULTS

Thermodynamic Analysis. (A) Noncomplementary Dodecamers. Short oligonucleotides usually undergo essentially a two-state melting transition that can be reliably monitored by hyperchromicity (UV melting) (*32*, *33*). We have used UV melting to determine the thermodynamic parameters (T_m, ΔH, and ΔG) of melting of the noncomplementary and self-complementary 12-mer DNA duplexes as a function of salt concentration and the number of pyrimidine bases modified at the 5 position. Figure 2A shows typical van't Hoff plots of modified noncomplementary oligonucleotides. The thermodynamic parameters are summarized in Table 1.

As the data show, the modifications increase the stability of the DNA duplex, with approximately a 2−3 K increase in T_m per modification at $I = 0.117$ M. This is further supported by the observation that the free energy change is a linear function of the number of modifications and that the curves for U, C dimethylamino and aminopropynyl modifications are essentially coincident (Figure 2B). The

slopes of these plots indicate a free energy increment of 3−3.5 kJ/mol per modification under these salt and pH conditions. The linearity suggests that the modifications are independent of one another, as expected given the spacing between modified bases in the molecule. In a B-DNA duplex, the amino nitrogen atoms are spaced at approximately 12 Å apart for modifications spaced at *i*, *i* + 2 (cf. the pdU) and 17 Å for the pdC spaced *i*, *i* + 4. As the groups are likely to be fully solvent exposed in the major groove (see below), the dielectric constant should be high, indicating only weak electrostatic interactions between adjacent groups. Nevertheless, the pronounced increase in stability afforded by the aminopropynyl modification requires a rationale.

The data for the dimethylaminopropynyl modification (Table 1) show at most a slight increase in stability over the free ammonium form. This suggests that the methyl groups are too far from the rest of the molecule to make any direct interactions, either with neighboring bases or with one another (and see below).

The data in Table 1 also indicate that the modifications increase the enthalpy difference between the duplex and strand states. The precision of ΔH is estimated to be around 5%, so the differences are somewhat marginal. However, if we assume that the U and C modifications are essentially equal, then on average each modification adds about 12.5 kJ·mol^{-1}·mod^{-1}. Thus, the energy terms can be approximated by the equations (all in kilojoules):

$$\Delta G(310) = 38.5 \pm 0.4 + (3.2 \pm 0.2)\ \text{nmod}$$

$$\Delta H = 355 \pm 12.5 + (12.5 \pm 4)\ \text{nmod}$$

$$\Delta S = 1.02 \pm 0.04 + (0.029 \pm 0.008)\ \text{nmod} \quad (10)$$

where nmod is the number of modifications (0, ..., 3).

To assess the electrostatic contribution to the duplex stability, and the influence of the charged modifications, we carried out UV melting studies at a fixed DNA concentration, as a function of total sodium concentration up to 1 M where the polyelectrolyte effects are essentially quenched (*24*). Figure 3 shows the variation of $\Delta G(310)$ with $\ln(a_{\pm})$. At low ionic strength, the free energy difference is essentially linear in $\ln(a_{\pm})$ but tails off at high ionic strength. Thus, salt stabilizes the duplex, as expected from ion condensation theory, but at high salt concentrations, additional effects that oppose the influence of the salt come into play. The slope of the line at low salt concentrations should be $d\Delta G/d \ln(a_{\pm}) = -RT(N/2)\Delta\zeta$, where N is the number of phosphate groups and $\Delta\zeta$ is the charge condensation parameter. If we assume structures appropriate for B-DNA and a random coil, $\Delta\zeta$ is about 0.27 at 310 K. Table 2 summarizes the slopes and apparent number of phosphates. In addition, the extrapolated value of $\Delta G(310)$ at 1 M ion activity is given and compared with the observed values. The values of N in Table 2 are generally close to the value expected for a pure B-DNA-coil transition, as there are 22 phosphates in a dodecamer. This indicates that despite the possible influence of end effects (*27*), the Record−Manning theory (*24*, *34*) reasonably well accounts for the polyelectrolyte effects in these duplexes. There is a general trend toward decreasing slope and therefore N value as the number of modifications increases. This indicates that the positive charges on the modified bases interact differently in the duplex and strand states and therefore influence the condensation properties. Because the N values decrease less than a full charge, this implies that either the conformation of the modified duplexes and/or strand states are affected by the modifications or that the charges interact in both states, albeit to different extents. The latter interpretation seems the more likely and suggests that electrostatics play some role in the stabilization by the charged aminopropynyl groups. This suggests that the amino

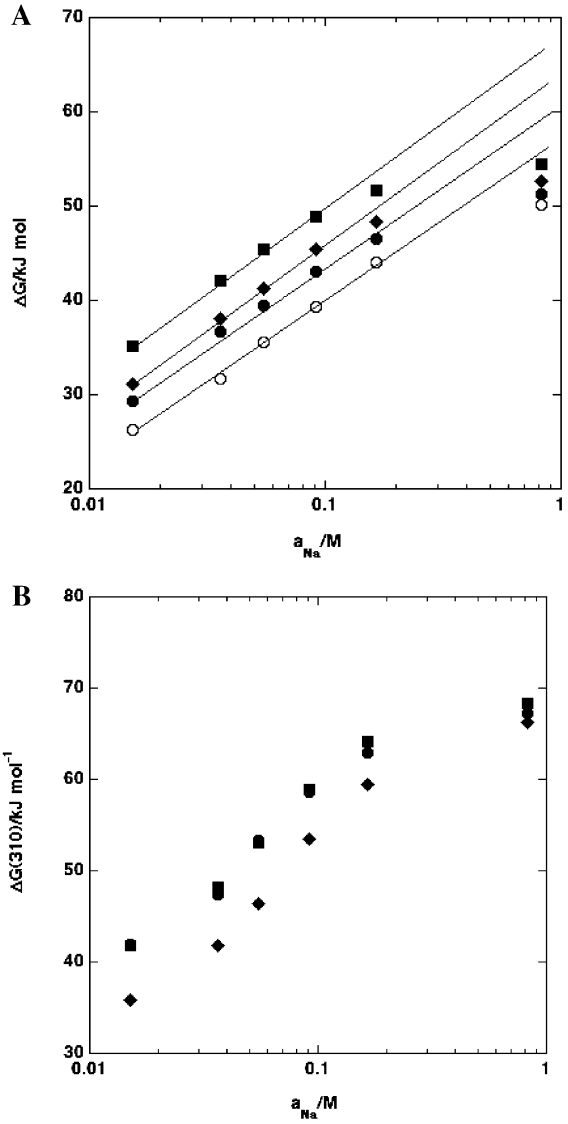

FIGURE 3: Dependence of free energy of dissociation on salt activity. The free energy change (dissociation) was calculated at 310 K as described in the text. (A) Noncomplementary duplexes: (○) unmodified; (●) aminopropynyl-T7; (◆) aminopropynyl-T7,T9; (■) aminopropynyl-T5,T7,T9. The lines represent the initial slopes $\partial \Delta G(310)/\partial \ln a$. (B) Complementary duplexes: (◆) native; (●) aminopropynyl-T7 (■); dimethylaminopropynyl-T7.

Table 2: Salt-Dependent Data for Noncomplementary Duplexes

no. of modifications	$\partial \Delta G(310)/\partial \ln a_{\pm}$ (kJ/mol)	ΔG(310, 1 M) (kJ/mol) calcd	ΔG(310, 1 M) (kJ/mol) obsd	N_{app}
0	7.49	57.3	50.5	20.6
1U	7.15	59.9	51.2	19.7
2U	7.32	62.2	52.7	20.2
3U	7.02	66.4	54.5	19.4
1C	7.39	60.0	51.2	20.5
2C	7.36	62.3	53.2	20.4
3C	6.86	65.5	57.1	18.9

group is fully charged at neutral pH and explains why the dimethyl modification has no additional stabilizing effect.

At 1 M salt, the polyelectrolyte effects are quenched, so that the free energy difference represents all of the nonpolyelectrolyte contributions to the stability. The difference in the ΔG(1 M) values between the modified duplexes and unmodified duplex is 2.7 ± 0.17 kJ·mol^{-1}·mod^{-1} for the line extrapolated to 1 M salt and 1.2 ± 0.4 kJ·mol^{-1}·mod^{-1} for the measured values at 1 M salt. The former value is the nonpolyelectrolyte effect from all sources, whereas the smaller value for the observed free energy differences is the nonpolyelectrolyte effect that is independent of additional indirect influence of ionic strength. Thus, there is a significant nonpolyelectrolyte effect, ca. 1.5 kJ·mol^{-1}·mod^{-1}, that at least indirectly depends on the salt activity.

There are several possible explanations for this effect. First, at sufficiently high concentrations of sodium, there may be site-specific binding in the minor groove, as suggested from high-resolution crystal structures (*35*). However, this would be expected to stabilize the duplex, which is opposite to the effect observed. Second, at low salt concentration, where the duplexes are relatively unstable, the melting is not pure two state, i.e., intermediates are present as the duplex unzips from the ends, and only at high concentrations of salt does the process become completely cooperative. In this interpretation, the free energy changes at 1 M salt would represent the true nonpolyelectrolye contribution, and at lower salt, there could be contributions from decreased cooperativity. Certainly, the melting curves show increasing baseline slopes at low salt concentrations, which could indicate non-two-state behavior (*18*−*20*).

Alternatively, as the activity of salt increases, the activity of water decreases. If there are changes in the amount of bound water between the duplex and strand state, then this will contribute to the entropy change. Duplex melting is associated with a release of approximately four water molecules per base pair (*28*); this would suggest a substantial influence of water activity on the stability. This is supported by recent quasielastic neutron scattering studies, which indicate a substantially larger amount of bound water in the duplex state than in the strand states of DNA (*36*). Further, as the water activity in 1 M sodium chloride is about 0.94, the release of 48 water molecules would destabilize a dodecamer by about 7.5 kJ/mol. This is close to the observed deviation between the linear extrapolation and the observed free energy change for the unmodified (control) duplex and suggests that hydration may be a significant contribution. As the deviation is larger for the modified duplexes, this would indicate that there is a greater release of water on dissociation for these duplexes; i.e., the modified duplexes are relatively more hydrated than the parent duplex.

(B) Self-Complementary Dodecamer. We have also examined the stabilization of a self-complementary duplex (the Drew−Dickerson dodecamer) bearing one modified thymine in each strand as a function of ionic strength. As Table 3 shows, the results are qualitatively the same as with the multiple modification data for the noncomplementary duplex and actually quantitatively similar when normalized on a per modification basis.

Figure 3B shows the variation of the free energy change as a function of salt concentration. As for the noncomplementary duplex, the free energy change is a linear function of ln($a_\pm$) at low salt but curves over at 1 M. The apparent number of phosphates was calculated from the slope of ΔG(310) versus the ion activity (Table 3). These are somewhat larger than for the noncomplementary duplex but show the same trend; N is smaller in the presence of the positively charged modifications. Furthermore, the extrapolated free energy change at 1 M shows a nonpolyelectrolyte contribution of 4.6 and 3.1 kJ/mol (2.3 and 1.5 kJ/mol modification) for the dimethylaminopropynyl and aminopropynyl groups, respectively. The dimethylamino modification is slightly more stable than the free amino form, as observed for the noncomplementary duplexes (see above). The observed free energy differences at 1 M salt are significantly smaller than the extrapolated values, 2.0 and 0.92 kJ/mol, respectively. Thus, there is a salt-dependent, nonelectrostatic effect on the stabilization, which could be attributed in significant measure to differences in the amount of water released on dissociation. We conclude that, as for the noncomplementary duplex, the modifications increase the thermodynamic stability by a combination of electrostatic effects, changing the hydration and other enthalpic effects such as altered base stacking.

Table 3: Thermodynamics of the ecoR1 Duplex at 0.117 M Ionic Strength[a]

modification	ΔH (kJ/mol)	ΔS [kJ/(mol·K)]	ΔG_{310} (kJ/mol)	T_m(2 μM) (K)
non	380 ± 19	1.05 ± 0.07	53.5 ± 1	327
T7 amino	380 ± 19	1.034 ± 0.08	58.9 ± 1.5	332
T7 dimethylamino	401 ± 20	1.10 ± 0.08	58.5 ± 1.5	331

[a] Thermodynamic parameters were obtained from curve fitting. Standard errors are estimated from the regression fits.

Table 4: Salt Dependence of ecoR1 Melting

molecule	$\partial \Delta G(310)/\partial \ln a_\pm$ (kJ/mol)	ΔG(310, 1 M) (kJ/mol) calcd	obsd	N_{app}
non	9.03 ± 0.7	72.4 ± 2	66.3	24.9 ± 2.1
T7 amino	8.57 ± 0.4	77.0 ± 1.3	68.3	23.6 ± 1.2
T7 dimethylamino	8.2 ± 0.6	75.6 ± 1.7	67.2	22.6 ± 1.6

Structural data are required to determine the origins of the polyelectrolyte and nonpolyelectrolyte contributions. We have therefore used high-resolution NMR and molecular modeling to evaluate the influence of the modification on structure and properties of the duplexes and isolated strand.

Conformational Analysis. To simplify the NMR spectra and conformational analysis, we have compared the effects of aminopropynyl and dimethylaminopropynyl modifications on the Drew−Dickerson dodecamer, whose solution conformation and chemical shift assignments are well documented (*37*−*40*). The ^{1}H chemical shifts were determined as described in the Methods.

Figure 4 shows the difference in chemical shifts between the aminopropynyl-derivatized sequence and the parent dodecamer recorded under nominally identical conditions (*38*). Unsurprisingly, the greatest shift perturbations occur for the H6 and HN3 of the modified base. However, other shift perturbations that are much larger than the noise are observed for the adjacent bases and sugars, namely, T7 and C9. This indicates that there are local perturbations in the neighborhood of the modified bases that are not transmitted more than one base pair beyond the altered sites.

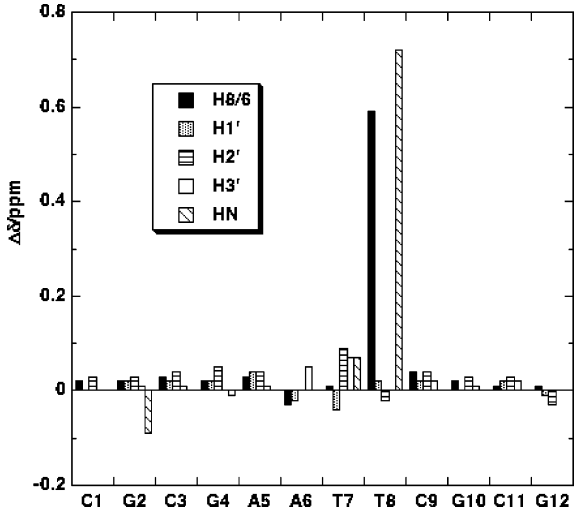

FIGURE 4: Chemical shift differences for the aminopropynyl-modified ecoR1 duplex. Chemical shifts were referenced to DSS at 30 °C. The chemical shifts of the native dodecamer were taken from ref *38*. Chemical shifts (error $<\pm 0.01$ ppm) were obtained from NOESY in D_2O and in H_2O and DQF-COSY experiments in D_2O. Shift differences were calculated for modified minus native sequences.

A similar profile was also observed for the dimethylamino derivative with somewhat larger shift perturbations. The lack of any NOEs connecting the methyl groups of the dimethylaminopropynyl-dU and the rest of the DNA suggests that they are far out in the major groove and exposed to solvent (not shown).

We have also determined the ^{13}C shifts of the sugars using HSQC; unlike the proton shifts there were no significant differences in the carbon frequencies (data not shown), with the exception of the aminopropynyl CH_2 group itself, which is substantially different for the two molecules.

The NOE intensities characteristic of base stacking geometry (base−base NOEs and sequential sugar−base NOES) and those that report on the nucleotide conformations (e.g., base−intraresidue sugar NOEs) are unaffected within experimental error, implying that there are only small changes in conformation of the nucleotides in the duplex state.

Sugar Conformations from Scalar Coupling Data. Scalar couplings can be used to determine the pseudorotation parameters of the deoxyriboses (*29*, *41*, *42*). We have recorded high digital resolution DQF-COSY spectra of the duplexes (Figure 5) and analyzed the sugar conformation as previously described (*29*). The DQF-COSY spectrum shows only small changes in coupling constants that are within experimental error (see Table 3). Hence the modifications have no major effect on the sugar conformations. The coupling data and NOEs also imply that all γ torsion angles are in the normal g^+ rotamer.

^{31}P NMR. The thermodynamic analysis showed a contribution to the duplex stability from electrostatic effects. This must involve the phosphodiester backbone, and ^{31}P NMR is sensitive to conformation and electrostatic effects (*43*−*45*). We have therefore assigned the ^{31}P NMR spectrum of the modified dodecamers and compared them with the free unmodified duplex previously assigned (*38*, *46*, *47*). Figure 6 shows the ^{31}P NMR chemical shift difference for the two modified duplexes. The ends (1−3 and 10−12) are unaffected by the modifications. The largest perturbations are for T8p and C9p, i.e., the two phosphodiesters flanking the modified base. However, there are also phosphate shift changes for A5 and A6. Although the shift perturbations are qualitatively similar, the dimethyl group seems to perturb the spectra more than the free amino group. The observed profile suggests possible direct effects of the positively charged group on the nearest phosphate but also some transmitted effects. As will be shown below, the amino group of the propynyl side chain is able to make simultaneous van der Waals and electrostatic interactions with the phosphate oxygens of T8 and C9, which probably accounts for the shift perturbations of these residues. The methyl groups on the nitrogen may require some conformational readjustment of the phosphodiester backbone to accommodate the extra bulk, which could be propagated across the base pairs to A5 and G4.

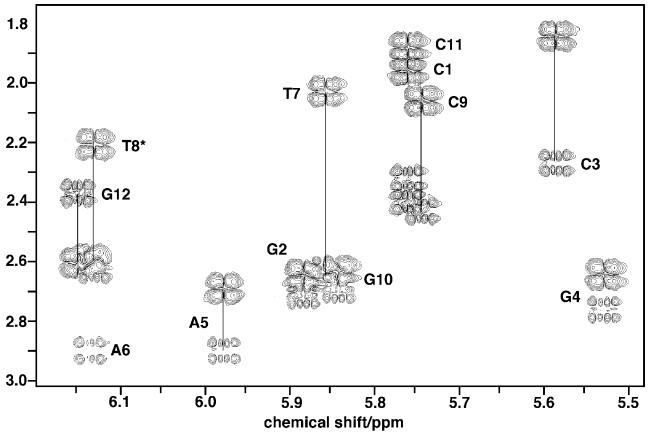

FIGURE 5: High-resolution DQF-COSY spectrum of ecoR1 with dimethylaminopropynyl. The spectrum was recorded at 14.1 T, 30 °C, with an acquisition time of 0.74 s in t_2 and 0.055 s in t_1. The data table was zero-filled to 16 K by 2 K before Fourier transformation, giving digital resolutions of 0.67 Hz/point in F_2 and 5.37 Hz/point in F_1. The region shows the scalar coupling between H1′ and H2′/H2″ for each residue.

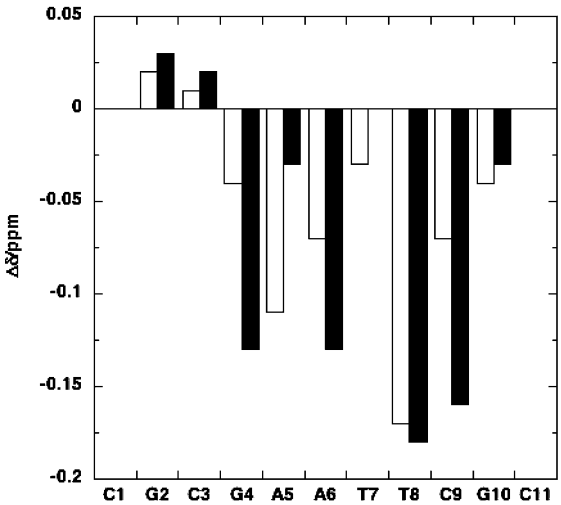

FIGURE 6: ^{31}P chemical shift differences in the modified ecoR1 dodecamer. $^{31}P-^{1}H$ HSQC spectra were recorded at 30 °C at 14.1 T on a 5 mm HCP probe with acquisition times of 0.4 s in t_2 and 0.1 s in t_1, respectively. Chemical shifts were assigned from the cross-peaks with H3′ (residue *i*) and H4′ (residue $i + 1$). Difference chemical shifts were obtained using the published values for the unmodified duplex at 30 °C. Key: (□) aminopropynyl-T7; (■) dimethylaminopropynyl-T7.

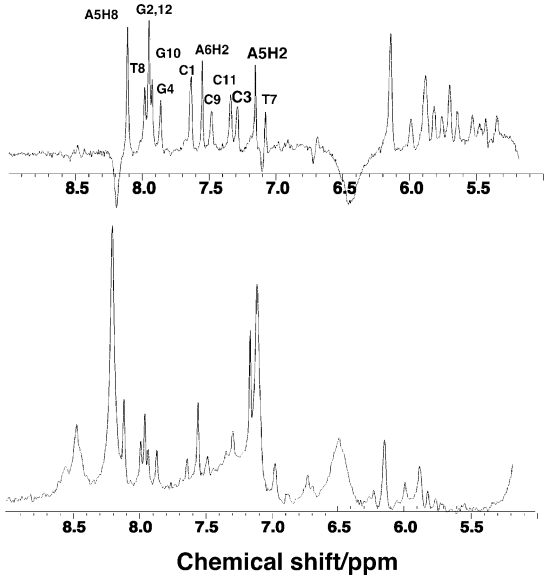

FIGURE 7: Hydration of the dimethylaminopropynyl ecoR1 dodecamer. Spectra were recorded at 800 MHz, 5 °C, with acquisition times of 0.256 s in t_2 and 21 ms in t_1, respectively. The solvent peak was suppressed using a Watergate sequence with flip back. Data were processed after zero filling to 16384 points in t_2 and 4096 points in t_1 and apodizing using a Gaussian function with 1 Hz line broadening exponential in each dimension prior to Fourier transformation. Upper spectrum: ROESY with a mixing time of 20 ms. Lower spectrum: NOESY with a mixing time of 40 ms.

Hydration of the Modified Duplexes Monitored by NMR. Water molecules that have a sufficiently long residence time to develop an NOE can be detected in NOESY and ROESY experiments (*30*, *48*, *49*). For example, the spine of hydration in the minor groove of the ecoR1 dodecamer was verified by the presence of water molecules close to the two adenine C2H, having a residence time in excess of 1 ns (*49*). We have recorded NOESY and ROESY spectra of the modified ecoR1 dodecamers at 14.1 and 18.8 T and at temperatures between 5 and 10 °C, with short mixing times. Figure 7 shows cross sections at the water frequency from ROESY and NOESY spectra recorded with 20 and 40 ms, respectively, at 5 °C and 800 MHz. The spectra show the negative NOEs (positive peaks, lower spectrum) and exchange cross-peaks for cytosine amino groups (negative peaks in the upper ROESY spectrum). In addition to the significant NOEs to the Ade C2H, there are also NOEs to H1′ resonances, some of which may arise from spin diffusion from the H3′ of resonances coincident with the water frequency (A6 and G2 at this temperature). In addition to these minor groove protons, there are also significant NOEs and ROEs to cytosine H5, H6, and H8. Most nonterminal bases show moderate or weak dipolar interactions with water; only A6H8 and T7H6 showed no cross-peak. A similar pattern of cross-peaks was observed for both the aminopropynyl and the dimethyaminopropynyl derivatives.

These results are consistent with there being somewhat stronger hydration in the modified duplexes. This supports the thermodynamic analysis above in that the modified duplexes are more hydrated than the unmodified duplex, leading to more water release on melting of the modified duplexes than the parent duplex.

Properties of the Single Strands. We have recorded NMR spectra of the modified and unmodified DNA strand (sequence 1; see Materials and Methods). Although the chemical shift dispersion is low, it was possible to assign the majority of base and sugar protons because of sequential NOEs including between neighboring bases. This indicates that there must be significant local helical stacking between neighboring bases. The intra and sequential base−sugar NOEs are indicative of glycosyl torsions in the high anti range (on average) and a right-handed helical twist. Furthermore, the observation of two strong cross-peaks for H1′−H2′/H2″ in the DQF-COSY spectrum (not shown) suggests that the sugars are predominantly in the C2′-endo domain. Furthermore, 1D NMR spectra showed substantial changes in line widths and chemical shifts as the temperature was varied over the range 10−50 °C. Spectra recorded in ^1H_2O at 10 °C showed only weak exchangeable proton resonances near 10 ppm, which are characteristic of imino protons in unpaired bases. Thus, there is no evidence for any hairpin of duplex formation in the strands.

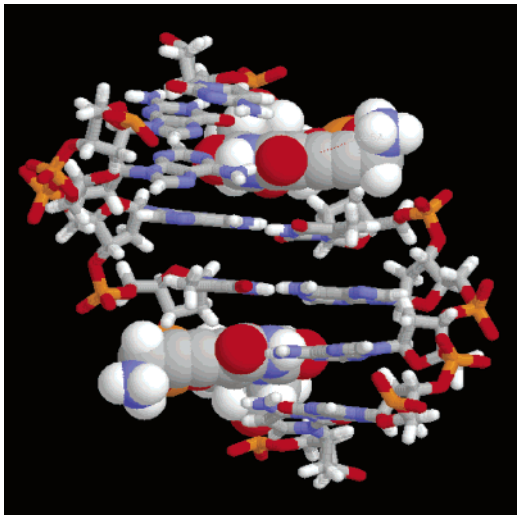

FIGURE 8: Model structures of aminopropynyl-modified ecoR1 dodecamer DNA. Models were built and minimized as described in the text. Only the central region is shown for clarity. The two symmetry-related aminopropynyl-dU residues are shown as space-filling structures. The amino group is in the lowest energy position and is available for interaction with solvent and making Coulombic interactions with the phosphodiester oxygen.

The major differences in chemical shift between the modified and unmodified strands arise, as expected, for the H6 of the modified bases, and which are comparable to those observed in the ecoR1 duplexes. Substantial changes in shift were also observed for the sugar protons of the modified nucleotide. The shift difference, in the direction of increased deshielding in the modified base, can be attributed to changes in electron density in the ring and/or local anisotropy effects from the propynyl triple bond. However, the base carbons also show large (8 ppm) downfield shifts for the C6 of the modified bases, suggesting that in part the difference does arise from changes in ring electron density.

Molecular Models. Figure 8 shows the relative placement of the aminopropynyl group in the major groove of the Dickerson−Drew dodecamer. The single degree of torsional freedom for the group was systematically varied. At the optimal position for interaction with the phosphate, the amine of the aminopropynyl group is 4.2 and 4.0 Å to the (*i*), (*i* − 1) closest phosphate oxygen, respectively. This is too far for a direct hydrogen bond between the two charge centers,

but an electrostatic interaction is significant. This close proximity to the phosphate groups in the major groove would stabilize the positive charge on the amine group. However, the lowest energy conformation does not have the protonated nitrogen associated with the (*i*), (*i* − 1) phosphates. In this conformation, the protonated amine points away from the phosphate groups. From a conformational point of view a single water molecule can bridge the charged amine group to the phosphate backbone in the (*i*) and (*i* − 1) positions [N to Owater 2.8 Å, Owater to OPhosphate 2.7 Å for (*i*) and (*i* − 1) positions]. These distances are also possible for the dimethylamine as the methyl groups do not have any direct van der Waals clashes with the neighboring environment. However using the modeling protocol the water molecules do not stay attached during the molecular dynamics, which is not surprising as full solvation calculations will be needed. This suggests the possibility of stabilization of the strand and may in part account for the observed changes in ^{31}P NMR chemical shifts (see above). The propynyl moiety also lies directly below the ring of the preceding thymine in the ecoR1 dodecamer (Figure 8) and could therefore make favorable stacking interactions.

DISCUSSION

The thermodynamic data show that the propynyl amino groups stabilize DNA duplexes both by electrostatic effects and by other contributions. We have been able to parse some of the contributions. Thus at 1 M salt, it is clear that the nonpolyelectrolyte effect amounts to about 2.5 kJ/mol per modification, with little difference between dU and dC. The polyelectrolyte theory holds reasonably well for these oligonucleotides; the small discrepancies from theory for the actual numbers of phosphates may reflect the deviations due to a combination of end effects and that such molecules are not perfect cylinders. However, the differences that we find due to the modifications are likely to be representative.

Approximately half of the observed nonpolyelectrolyte contribution arises from indirect ion-dependent effects, which we attribute largely to hydration. The modified bases are either more hydrated in the duplex and/or less hydrated in the strand state than either dT or dC. The polyelectrolyte effect, which is manifested at physiological concentration of salt, is modest and at 117 mM sodium amounts to around 2 kJ·mol^{-1}·mod^{-1}. The modifications also are enthalpically stabilizing, which are in part offset by the unfavorable entropy of hydration of the duplex compared with the strands. Methylation of the amino group caused a slight further increase in stability.

NMR spectroscopy of the modified duplexes showed that as far as base stacking and nucleotide conformation is concerned these modifications have minimal effects on conformation of the duplex. Also, the single strands are helically stacked with small effects on adding the aminopropyne group. The modifications place a positive charge between adjacent phosphate groups in a strand, which may serve to stabilize the local helical character, or preorganize the strands. This is supported by the increased propensity for stacking in the modified strands and the perturbation of the ^{31}P NMR spectra in the DNA duplexes. The electrostatic clamp seems to propagate across the base pair and may increase local stacking interactions. The presence of charge between phosphates may also interfere with local ion condensation, in accordance with the salt dependence of the stability of these modified duplexes.

The altered electronic structure of the modified bases shown by the absorbance and NMR spectra implies an alteration of the dipole moment, which may improve nearest neighbor stacking energies, and could contribute to the favorable enthalpy change associated with the modifications. The sequential base−base NOEs in the modified strand are in general somewhat stronger than in the unmodified strand, as are the characteristic helical base−sugar NOEs, suggesting a slightly greater propensity for helical stacking in the modified strand than in the unmodified strand. This could contribute favorably to the net free energy difference.

We have shown by parsing the energy contributions that electrostatic (and perhaps electronic) and hydration effects can produce substantial increases in thermodynamic stability without significant changes in the conformation of the duplex state.

ACKNOWLEDGMENT

We thank Dr. J. B. Chaires for valuable discussions about the manuscript.

SUPPORTING INFORMATION AVAILABLE

Details of the chemical synthesis of the aminopropynyl nucleotides and tables of chemical shifts of modified DNA duplexes and single strands. This material is available free of charge via the Internet at http://pubs.acs.org.

REFERENCES

1. Lesnik, E. A., and Freier, S. M. (1995) Relative thermodynamic stability of DNA, RNA, and DNA-RNA hybrid duplexes—Relationship with base composition and structure, *Biochemistry 34*, 10807−10815.
2. Flanagan, W. M., Wolf, J. J., Olson, P., Grant, D., Lin, K. Y., Wagner, R. W., and Matteucci, M. D. (1999) A cytosine analog that confers enhanced potency to antisense oligonucleotides, *Proc. Natl. Acad. Sci. U.S.A. 96*, 3513−3518.
3. Barnes, T. W., and Turner, D. H. (2001) C5-(1-Propynyl)-2′-deoxypyrimidines enhance mismatch penalties of DNA:RNA duplex formation, *Biochemistry 40*, 12738−12745.
4. Barnes, T. W., and Turner, D. H. (2001) Long-range cooperativity in molecular recognition of RNA by oligodeoxynucleotides, with multiple C5-(1-propynyl pyrimidines, J. *Am. Chem. Soc. 123*, 4107−4118.
5. Wagner, R. W., Matteucci, M. D., Grant, D., Huang, T., and Froehler, B. C. (1996) Potent and selective inhibition of gene expression by an antisense heptanucleotide, *Nat. Biotechnol. 14*, 840−844.
6. Bijapur, J., Keppler, M. D., Bergqvist, S., Brown, T., and Fox, K. R. (1999) 5-(1-Propargylamino)-2′-deoxyuridine (U-P): a novel thymidine analogue for generating DNA triplexes with increased stability, *Nucleic Acids Res. 27*, 1802−1809.
7. Gyi, J. I., Gao, D., Conn, G. L., Trent, J. O., Brown, T., and Lane, A. N. (2003) The solution structure of a DNA·RNA duplex containing 5-propynyl U and C; comparison with 5-Me modifications, *Nucleic Acids Res. 31*, 2683−2693.
8. Gowers, D. M., Bijapur, J., Brown, T., and Fox, K. R. (1999) DNA triple helix formation at target sites containing several pyrimidine interruptions: stabilization by protonated cytosine or 5-(1-propargylamino), *Biochemistry 38*, 13747−13758.
9. Mills, M., Arimondo, P. B., Lacroix, L., Garestier, T. S., Klump, H., and Mergny, J. L. (2002) Chemical modification of the third strand: Differential effects on purine and pyrimidine triple helix formation, *Biochemistry 41*, 357−366.
10. Phipps, A. K., Tarkoy, M., Schultze, P., and Feigon, J. (1998) Solution structure of an intramolecular DNA triplex containing

5-(1-propynyl)-2′-deoxyuridine residues in the third strand, *Biochemistry 37*, 5820−5830.
11. Lacroix, L., Lacoste, J., Reddoch, J. F., Mergny, J. L., Levy, D. D., Seidman, M. M., Matteucci, M. D., and Glazer, P. M. (1999) Triplex formation by oligonucleotides containing 5-(1-propynyl)-2′-deoxyuridine: Decreased magnesium dependence and improved intracellular gene targeting, *Biochemistry 38*, 1893−1901.
12. Sollogoub, M., Richard, A. J., Darby, R. A. J., Cuenoud, B., Brown, T., and Fox, K. R. (2002) Stable DNA triple helix formation using oligonucleotides containing 2′-aminoethoxy,5-propargylamino-U, *Biochemistry 41*, 7224−7231.
13. Cruickshank, K. A., and Stockwell, D. L. (1988) Oligonucleotide labeling—a concise synthesis of a modified thymidine phosphoramidite, *Tetrahedron Lett. 29*, 5221−5224.
14. Heystek, L. E., Zhou, H. Q., Dande, P., and Gold, B. (1998) Control over the localization of positive charge in DNA: The effect on duplex DNA and RNA stability, *J. Am. Chem. Soc. 120*, 12165−12166.
15. Seela, F., Ramzaeva, N., Leonard, P., Chen, Y., Debelak, H., Feiling, E., Kroschel, R., Zulauf, M., Wenzel, T., Frohlich, T., and Kostrzewa, M. (2001) Phosphoramidites and oligonucleotides containing 7-deazapurines and pyrimidines carrying aminopropargyl side chains, *Nucleosides, Nucleotides Nucleic Acids 20*, 1421−1424.
16. Ahmadian, M., Zhang, P. M., and Bergstrom, D. E. (1998) A comparative study of the thermal-stability of oligodeoxyribonucleotides containing 5-substituted 2′ deoxyuridines, *Nucleic Acids Res. 26*, 3127−3135.
17. Chalikian, T. V., Völker, J., Plum, G. E., and Breslauer, K. J. (1999) A more unified picture for the thermodynamics of nucleic acid duplex melting: a characterisation by calorimetric and volumetric techniques, *Proc. Natl. Acad. Sci. U.S.A. 96*, 7853−7858.
18. Holbrook, J. A., Capp, M. W., Saecker, R. M., and Record, M. T. (1999) Enthalpy and heat capacity changes for formation of an oligomeric DNA duplex: interpretation of coupled processes of formation and association of single-stranded helices, *Biochemistry 38*, 8409−8422.
19. Jelesarov, I., Crane-Robinson, C., and Privalov, P. L. (1999) The energetics of HMG box interactions with DNA: thermodynamic description of the target DNA duplexes, *J. Mol. Biol. 294*, 981−995.
20. Lane, A. N., and Jenkins, T. C. (2000) Thermodynamics of nucleic acids and their interactions with ligands, *Q. Rev. Biophys. 33*, 255−306.
21. Rouzina, I., and Bloomfield, V. A. (1999) Heat capacity effects on the melting of DNA. 1. General aspects, *Biophys. J. 77*, 3242−3251.
22. Rouzina, I., and Bloomfield, V. A. (1999) Heat capacity effects on the melting of DNA. 2. Analysis of nearest-neighbor base-pair effects, *Biophys. J. 77*, 3252−3255.
23. McDowell, J. A., and Turner, D. H (1996) Investigation of the structural basis for thermodynamic stabilities of tandem GU mismatches: Solution structure of (rGAGGUCUC)(2) by two-dimensional NMR and simulated annealing, *Biochemistry 35*, 14077−14089.
24. Record, M. T., Anderson, C. F., and Lohman, T. M. (1978) Thermodynamic analysis of ion effects on binding and conformational equilibria of proteins and nucleic-acids—Roles of ion association or release, screening, and ion effects on water activity, *Q. Rev. Biophys. 11*, 103−178.
25. Anderson, C. F., and Record, M. T. (1990) ion distributions around DNA and other cylindrical polyions—Theoretical descriptions and physical implications, *Annu. Rev. Biophys. Biophys. Chem. 19*, 423−465.
26. Anderson, C. F., and Record, M. T. (1995) Salt nucleic-acid interactions, *Annu. Rev. Phys. Chem. 46*, 657−700.
27. Shkel, I. A., and Record, M. T., Jr. (2004) Effect of the number of nucleic acid oligomer charges on the salt dependence of stability ($\Delta G°37$) and melting temperature (*T*m): NLPB analysis of experimental data, *Biochemistry* (in press).
28. Spink, C. H., and Chaires, J. B. (1999) Effects of hydration, ion release, and excluded volume on the melting of triplex and duplex DNA, *Biochemistry 38*, 496−508.
29. Conte, M. R., Bauer, C. J., and Lane, A. N. (1996) Determination of sugar conformations by NMR in larger DNA duplexes using both dipolar and scalar data: application to d(CATGTGACGT-CACATG)$_2$, *J. Biomol. NMR 7*, 190−206.
30. Lane, A. N., Jenkins, T. C., and Frenkiel, T. A. (1997) Hydration and solution structure of d(CGCAAATTTGCG)$_2$ and its complex with propamidine from NMR and molecular modelling, *Biochim. Biophys. Acta 1350*, 189−204.
31. Mohamadi, F., Richards, N. G. I., Guida, W. C., Liskamp, R., Lipton, M., Caufield, C., Chang, G., Hendrickson, T, and Still, W. C. (1990) MacroModel—an integrated software mechanics, *J. Comput. Chem. 11*, 440−455.
32. Turner, D. H. (1996) Thermodynamics of base pairing, *Curr. Opin. Struct. Biol. 6*, 299−304.
33. SantaLucia, J., Jr., Allawi, H. T., and Seneviratne, P. A. (1996) Improved nearest-neighbor parameters for predicting DNA duplex stability, *Biochemistry 35*, 3555−3562.
34. Manning, G. S. (1978) Molecular theory of polyelectrolyte solutions with applications to electrostatic properties of polynucleotides, *Q. Rev. Biophys. 11*, 179−246.
35. Shui, X. Q., McFail-Isom, L., Hu, G. G., and Williams, L. D. (1998) The B-DNA dodecamer at high resolution reveals a spine of water on sodium *Biochemistry 37*, 8341−8355.
36. Bastos, M., Castro, V., Mrevlishvili, G., and Teixeira, J. (2004) Hydration of ds-DNA and ss-DNA by neutron quasielastic scattering, *Biophys. J. 86*, 3822−3827.
37. Hare, D. R., Wemmer, D. E., Chou, S. H., Drobny, G., and Reid, B. R. (1983) Assignment of the non-exchangeable proton resonances of d(C-G-C-G-A-A-T-T-C-G-C-G) using two-dimensional nuclear magnetic-resonance methods, *J. Mol. Biol. 171*, 319−336.
38. Lane, A. N., Jenkins, T., Brown, T., and Neidle, S. (1991) Conformation of the *eco* R1 dodecamer in solution and its interaction with the minor groove binding drug Berenil, *Biochemistry 30*, 1372−1385.
39. Tjandra, N., Tate, S., Ono, A., Kainosho, M., and Bax, A. (2000) The NMR structure of a DNA dodecamer in an aqueous dilute liquid crystalline phase, *J. Am. Chem. Soc. 122*, 6190−6200.
40. Wu, Z. G., Delaglio, F., Tjandra, N., Zhurkin, V. B., and Bax, A. (2003) Overall structure and sugar dynamics of a DNA dodecamer from homo and heteronuclear dipolar couplings and P-31 chemical shift anisotropy, *J. Biomol. 26*, 297−315.
41. Van Wijk, J., Huckriede, B. D., Ippel, J. H., and Altona, C. (1992) Furanose sugar conformations in DNA from NMR coupling-constants, *Methods Enzymol. 211*, 286−306.
42. Schmitz, U., Sethson, I., Egan, W. M., and James, T. L. (1992) Solution structure of a DNA octamer containing the Pribnow box via restrained molecular-dynamics simulation with distance and torsion angle constraints derived from 2-dimensional nuclear-magnetic-resonance spectral fitting, *J. Mol. Biol. 227*, 510−531.
43. Gorenstein, D. G. (1984) *Phosphorus P-31 NMR: Principles and Applications*, Academic Press, Orlando, FL.
44. Ebel, S., Brown, T., and Lane, A. N. (1994) Thermodynamic stability and solution conformation of tandem G.A mismatches in RNA and RNA·DNA hybrid duplexes, *Eur. J. Biochem. 220*, 703−715.
45. Legault, P., and Pardi, A. (1994) P-31 chemical-shift as a probe of structural motifs in RNA, *J. Magn. Reson. B 103*, 82−86.
46. Wu, Z., Tjandra, N., and Bax, A. (2001) ^{31}P chemical shift anisotropy as an aid in determining nucleic acid structure in liquid crystals, *J. Am. Chem. Soc. 123*, 3617−3618.
47. Ott, J., and Eckstein, F. (1985) P-31 NMR spectral-analysis of the dodecamer d(CGCGAATTCGCG), *Biochemistry 24*, 2530−2535.
48. Liepinsh, E., Otting, G., and Wuthrich, K. (1992) NMR observation of individual molecules of hydration water bound to dna duplexes—Direct evidence for a spine of hydration water present in aqueous-solution, *Nucleic Acids Res. 20*, 6549−6553.
49. Liepinsh, E., Leupin, W., and Otting, G. (1994) Hydration of DNA in aqueous-solution—NMR evidence for a kinetic destabilization of the minor-groove hydration of d-(TTAA)(2) versus D-(AATT)-(2) segments, *Nucleic Acids Res. 22*, 2249−2254.

BI047561D